Contribution from the Department of Chemistry,
McMaster University, Hamilton, Ontario L8S 4M1, Canada

Crystal Structure, Raman, and Multinuclear Magnetic Resonance Study of $FXeN(SO_2F)_2$, an Example of Xenon–Nitrogen Bonding

JEFFERY F. SAWYER, GARY J. SCHROBILGEN,* and STEVEN J. SUTHERLAND

Received February 10, 1982

The crystal structure of fluoro[imidobis(sulfuryl fluoride)]xenon(II) has been determined at −55 °C from three-dimensional X-ray data. The compound crystallizes in the monoclinic system, space group $P2_1/a$, with four molecules in a unit cell of dimensions a = 11.827 (4) Å, b = 6.828 (2) Å, c = 9.467 (3) Å, and β = 112.65 (2)°. The structure was solved by the heavy-atom method and refined by least-squares and Fourier methods to a final R factor of 0.023 for 1721 observed ($F > 6\sigma(F)$) reflections. The structure analysis has established the existence of discrete $FXeN(SO_2F)_2$ molecules and shows that $FXeN(SO_2F)_2$ is Xe–N bonded, representing the first definitive proof for the existence of the Xe–N bond. The xenon atom is approximately linearly coordinated by the nitrogen atom of the imidobis(sulfuryl fluoride) group and a fluorine atom. The angle F–Xe–N is 178.1 (1)°, and the interatomic distances are Xe–N = 2.200 (3) Å and Xe–F = 1.967 (3) Å. Raman spectral data and assignments are also presented for $FXeN(SO_2F)_2$, $HN(SO_2F)_2$, and $Cs^+N(SO_2F)_2^-$. Solution ^{15}N, ^{129}Xe, and ^{19}F NMR studies of ^{15}N-enriched $FXeN(SO_2F)_2$ demonstrate that $FXeN(SO_2F)_2$ is also Xe–N bonded in solution. The first example of a directly bonded ^{129}Xe–^{15}N coupling (305 Hz) is also reported.

Introduction

Xenon compounds containing either xenon–fluorine or xenon–oxygen bonds have been known since the inception of noble-gas chemistry. It is only more recently, however, that the syntheses of xenon compounds containing nitrogen have been reported. Previous reports of compounds formulated as $FXeN(SO_2F)_2$[1a,b] and $F[XeN(SO_2F)_2]_2^+AsF_6^-$[1b,c] have claimed that both species contain xenon bonded to nitrogen. These claims are based primarily on ^{19}F NMR results which are consistent with the proposed Xe–N-bonded structures but do not represent unique interpretations. It has been pointed out, for example, that the ^{19}F (and ^{129}Xe) solution NMR spectrum of $FXeN(SO_2F)_2$ could also be interpreted in terms of a structure in which the Xe–F group undergoes a rapid intramolecular exchange over the nitrogen and/or oxygen sites.[2] Similarly, the ^{19}F NMR spectrum of $F[XeN(SO_2F)_2]_2^+$ in BrF_5 as solvent suggests that the cation is partially dissociated,[1b,c] and the ensuing chemical exchange permits neither the observation of the bridging fluorine resonance nor any definitive conclusions to be made about the xenon bonding site in the cation. A detailed solution NMR study of $Xe[N(SO_2F)_2]_2$ (the compound was also reported by DesMarteau et al.[1b]), is the subject of a subsequent paper[3] and demonstrates that this compound contains xenon bonded to two nitrogens. In view of the fact that no clear structural evidence existed to unequivocally support either Xe–N- or Xe–O-bonded structures for $FXeN(SO_2F)_2$ or $F[XeN(SO_2F)_2]_2^+$, we have obtained a low-temperature X-ray crystal structure of the title compound and its ^{15}N NMR parameters in solution for the first time. These results were the subject of a recent preliminary communication.[4] In the present paper we describe, in detail, the definitive characterization of the first example of an Xe–N-bonded compound, $FXeN(SO_2F)_2$, both in the solid state and in solution.

Results and Discussion

Crystal Structure. The structural analysis shows that crystals of $FXeN(SO_2F)_2$ consist of an ordered assembly of discrete molecules (illustrated in Figure 1) in which the xenon atom of the Xe–F group is bonded to the nitrogen atom of the ligand. This structure gives the first definitive proof for the existence of a stable xenon–nitrogen bond and supports the earlier view that this compound is Xe–N bonded.[1a,b] The bond distance, bond angles, and selected intra- and intermolecular contacts are given in Table I. A view of the $FXeN(SO_2F)_2$ molecule indicating the atomic numbering scheme and some pertinent bond lengths is given in Figure 1.

Table I. Bond Lengths (Å), Bond Angles (Deg), and Some Significant Contact Distances (Å) for $FXeN(SO_2F)_2$[a]

Bond Lengths			
Xe–F	1.967 (3)	N–S(1)	1.628 (3)
–N	2.200 (3)	–S(2)	1.623 (3)
···O(13)	3.178 (3)	S(1)–F(11)	1.539 (3)
···O(23)	3.201 (3)	–O(12)	1.405 (4)
···O(21)^{I}	3.381 (3)	–O(13)	1.401 (3)
···O(21)^{II}	3.594 (3)	S(2)–F(21)	1.532 (3)
···O(23)^{II}	3.473 (3)	–O(22)	1.402 (3)
···F^{III}	3.294 (3)	–O(23)	1.410 (3)
···O(12)^{IV}	3.386 (3)		
···O(23)^{V}	3.487 (3)		

Bond Angles			
F–Xe–N	178.1 (1)	Xe–N–S(1)	119.3 (2)
F–Xe–O(13)	130.6 (1)	–S(2)	120.1 (1)
–O(23)	129.7 (1)	S(1)–N–S(2)	120.5 (2)
–O(21)^{I}	63.9 (1)	N–S(1)–F(11)	101.0 (1)
–O(21)^{II}	72.6 (1)	–O(12)	110.8 (2)
–O(23)^{II}	106.5 (1)	–O(13)	107.0 (2)
–F^{III}	97.4 (1)	F(11)–S(1)–O(12)	105.8 (2)
–O(12)^{IV}	117.7 (1)	–O(13)	106.7 (2)
–O(23)^{V}	69.2 (1)	O(12)–S(1)–O(13)	123.3 (2)
N–Xe–O(13)	50.0 (1)	N–S(2)–F(21)	101.4 (1)
–O(23)	49.8 (1)	–O(22)	111.5 (2)
–O(21)^{I}	117.7 (1)	–O(23)	107.4 (2)
–O(21)^{II}	105.9 (1)	F(21)–S(2)–O(22)	106.5 (2)
–O(23)^{II}	71.7 (1)	–O(23)	106.1 (2)
–F^{III}	81.3 (1)	O(22)–S(2)–O(23)	121.9 (2)
–O(12)^{IV}	64.2 (1)		
–O(23)^{V}	110.7 (1)		

[a] Symmetry transformations are indicated by the following superscripts: (I) $x, -1+y, z$; (II) $-x, 2-y, -z$; (III) $^1/_2-x, {}^1/_2+y, -z$; (IV) $^1/_2-x, -{}^1/_2+y, 1-z$; (V) $^1/_2+x, {}^3/_2-y, z$.

The Xe–N and Xe–F distances in $FXeN(SO_2F)_2$ are 2.200 (3) and 1.967 (3) Å, respectively, and the F–Xe–N system is very nearly linear (∠F–Xe–N = 178.1 (1)°). The present Xe–F bond length is considerably longer than the terminal Xe–F bond lengths in $FXeOSO_2F$ (1.940 (8) Å),[5] $Xe_2F_3^+$

(1) (a) LeBlond, R. D.; Desmarteau, D. D. *J. Chem. Soc., Chem. Commun.* **1974**, 555. (b) Desmarteau, D. D.; LeBlond, R. D.; Hassain, S. F.; Nothe, D. *J. Am. Chem. Soc.* **1981**, *103*, 7734. (c) DesMarteau, D. D. *Ibid.* **1978**, *100*, 6270.
(2) Schrobilgen, G. J.; Holloway, J. H.; Granger, P.; Brevard, C. *Inorg. Chem.* **1978**, *17*, 980.
(3) Schrobilgen, G. J.; Schumacher, G. A., submitted for publication in *Inorg. Chem.*
(4) Sawyer, J. F.; Schrobilgen, G. J.; Sutherland, S. J. *J. Chem. Soc., Chem. Commun.* **1982**, 210.
(5) Bartlett, N.; Wechsberg, M.; Jones, G. R.; Burbank, R. D. *Inorg. Chem.* **1972**, *11*, 1124.

0020-1669/82/1321-4064$01.25/0

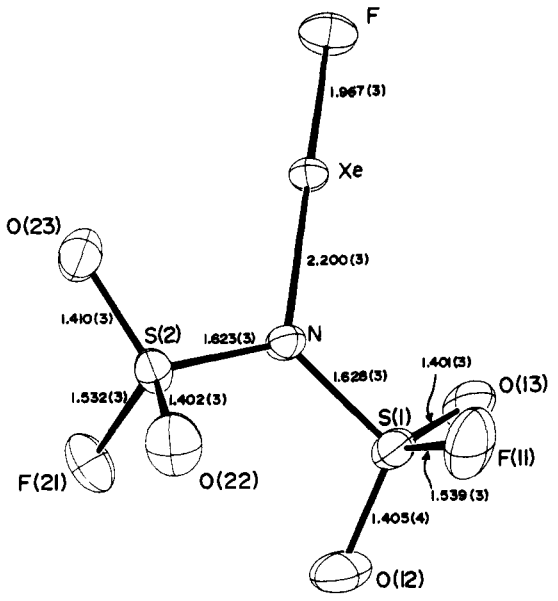

Figure 1. Perspective drawing of $FXeN(SO_2F)_2$ showing the numbering scheme and bond lengths (Å) (thermal ellipsoids are drawn at the 50% probability level).

(1.90 (2) Å, AsF_6^- salt),[6] and $(FXeO)_2SOF^+$ (1.86 (3) Å),[7] the fluorosulfate analogue of the $Xe_2F_3^+$ cation, and in XeF^+ salts with the anions RuF_6^- (1.87 (2) Å),[8] $Sb_2F_{11}^-$ (1.82 (3) Å),[9] and AsF_6^- (1.873 (6) Å)[10] but is still shorter than the Xe–F bonds in XeF_2 (2.01 (1) Å).[11] In comparison, the Xe–O distances of 2.155 (8) and 2.12 (5) Å in $FXeOSO_2F$[5] and $Xe(OSeF_5)_2$,[12] respectively, and the Xe···F bridge distance in FXe···$FRuF_5$ (2.18 (2) Å)[8] are all shorter than the Xe–N distance in $FXeN(SO_2F)_2$. The Xe–N bond length is, however, significantly shorter than the Xe···F bridge distances in FXe···FSb_2F_{10} (2.35 (2) Å)[9] and FXe···$FAsF_5$ (2.212 (5) Å)[10] and the Xe–O bonds in $(FXeO)_2SOF^+$ (2.22 (2) Å).[7] In all these latter compounds, the additional Xe–F or Xe–O interactions are always virtually collinear with the terminal Xe–F bond of the cation, consistent with the VSEPR rules[13] for the AX_2E_3 formulation of the central Xe(II) atom.

It is generally agreed that the Xe–F bond in XeF_2 is considerably less than an electron-pair bond. Both the simple molecular orbital bonding model[14] (three-center–four-electron bond description) and the valence bond treatment[15] depict the three atoms as bound by a single electron pair. As with the MO description, the valence bond description suggests a high bond polarity (i.e., the major canonical forms in the resonance hybrid are $F–Xe^+F^-$ and $F^-Xe^+–F$), yielding an Xe–F bond order of $^1/_2$. With use of the bond order–bond length relationship of Pauling,[16] for the calculation of terminal Xe–F bond orders, the present Xe–F bond has a bond order of 0.59. The Xe–F bond of $FXeN(SO_2F)_2$ is apparently the most XeF_2-like bond encountered thus far. As has been proposed for other xenon(II) compounds, the bonding description of $FXeN(SO_2F)_2$ can be represented as a resonance hybrid of valence bond structures I and II. Considering the long Xe–F bond,

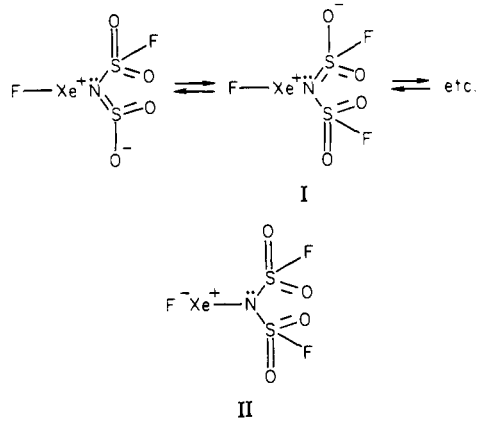

structure I apparently is not as important in the present compound as in other xenon(II) compounds. Our result for the Xe–F bond order implies that valence bond structure I only has a 59:41 dominance over valence bond structure II.

The imidobis(sulfuryl fluoride) geometry is also consistent with the partial ionic bonding discussed above. In the $N(SO_2F)_2$ group, the S–N distances of 1.623 (3) and 1.628 (3) Å are only slightly longer by ca. 0.40 Å than the longest S–N bond in the anion $[NSF_2NSO_2F]^-$ (1.587 (9) Å)[17] and are only slightly shorter than the S–N distances in compounds such as potassium sulfamate, $K[NH_2SO_3]$ (1.666 (6) Å),[18] potassium imidosulfonate, $K_2[NH(SO_3)_2]$ (1.674 (5) Å),[19] and potassium nitrilosulfonate, $K_3[N(SO_3)_3]\cdot 2H_2O$ (1.71 (2) Å).[20] All of these bonds are assumed to have some π-bond character resulting from overlap of the lone-pair orbital on nitrogen and the unfilled 3d orbitals of the sulfur atoms. In sulfamic acid, $H_3N^+SO_3^-$,[21] where there are no electrons on nitrogen available for π bonding, the S–N bond length of 1.772 Å is assumed to correspond to that for a single bond. The S–N distances in $FXeN(SO_2F)_2$ are also much shorter than the value of 1.74 Å calculated for a S–N single bond from Pauling's covalent radii. Thus it may be concluded that the S–N bonds in $FXeN(SO_2F)_2$ have considerable double-bond character. Several authors have proposed bond order–bond length correlations for S–N bonds, and with use of those of Nyburg[22a] and Gillespie[22b] the bond order for the S–N bonds in the present compound is calculated to be 1.45 and 1.30, respectively.

Considerations similar to those applied to the S–N bonds also apply for the S–O bonds, which are known to have an appreciable variation in bond lengths and bond orders. In $FXeN(SO_2F)_2$, however, the average S–O bond length of 1.404 (3) Å is significantly shorter than the S–O distances observed in examples of the fluorosulfate anion (e.g., 1.415 (3), 1.415 (3), and 1.419 (3) Å in $S_6N_4(SO_3F)_2$[23]) and the S–O distances

(6) Bartlett, N.; DeBoer, B. G.; Hollander, F. J.; Sladky, F. O.; Templeton, D. H.; Zalkin, A. *Inorg. Chem.* **1974**, *13*, 780.
(7) Gillespie, R. J.; Schrobilgen, G. J.; Slim, D. R. *J. Chem. Soc., Dalton Trans.* **1977**, 1003.
(8) Bartlett, N.; Gennis, M.; Gibler, D. D.; Morrell, B. K.; Zalkin, A. *Inorg. Chem.* **1973**, *12*, 1717.
(9) Burgess, J.; Fraser, C. J. W.; McRae, V. M.; Peacock, R. D.; Russell, D. R. *Inorg. Nucl. Chem., Suppl.* **1976**, 183.
(10) Zalkin, A.; Ward, D. L.; Biagioni, R. N.; Templeton, D. H.; Bartlett, N. *Inorg. Chem.* **1978**, *17*, 1318.
(11) Levy, H. A.; Agron, P. A. *J. Am. Chem. Soc.* **1963**, *85*, 240.
(12) Templeton, L. K.; Templeton, D. H.; Seppelt, K.; Bartlett, N. *Inorg. Chem.* **1976**, *15*, 2718.
(13) Gillespie, R. J. "Molecular Geometry"; Van Nostrand-Reinhold: London, 1972; pp 62–69.
(14) Rundle, R. A. *J. Am. Chem. Soc.* **1963**, *85*, 112.
(15) Coulson, C. A. *J. Chem. Soc.* **1964**, 1442.
(16) Pauling, L. "The Nature of the Chemical Bond", 3rd ed.; Cornell University Press: Ithaca, NY, 1960; p 255.
(17) Buss, B.; Altena, D.; Höfer, R.; Glemser, O. *J. Chem. Soc., Chem. Commun.*, **1978**, 226.
(18) (a) Jeffrey, G. J.; Stadler, J. *J. Chem. Soc.* **1951**, 1467. (b) Cox, G. W.; Sabine, T. M.; Padmanabhan, V. M.; Ban, N. T.; Chung, M. K.; Surjadi, A. S. *Acta Crystallogr.* **1967**, *23*, 578.
(19) (a) Jeffrey, G. J.; Jones, D. W. *Acta Crystallogr.*, **1956**, *9*, 283. (b) Hodgson, P. G.; Moore, F. H.; Kennard, C. H. L. *J. Chem. Soc., Dalton Trans.* **1976**, 1443.
(20) Tillack, J. V.; Kennard, C. H. L. *J. Chem. Soc. A* **1970**, 1637.
(21) Bats, J. W.; Coppens, P.; Koetzle, T. F. *Acta Crystallogr., Sect. B*, **1977**, *B33*, 37.
(22) (a) Nyburg, S. C. *J. Cryst. Mol. Struct.* **1973**, *3*, 331. (b) Gillespie, R. J.; Ireland, P. R.; Vekris, J. E. *Can. J. Chem.* **1975**, *53*, 3147.

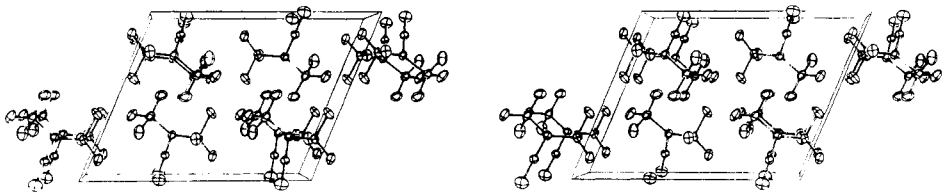

Figure 2. Stereoscopic view of the packing in the unit cell of $FXeN(SO_2F)_2$ viewed down the *b* axis.

in the $NH_2SO_3^-$ (1.457 Å),[18] $NH(SO_3)_2^{2-}$ (1.449 Å),[19] and $N(SO_3)_3^{3-}$ (1.468 Å)[20] anions. These values indicate that the S–O bonds in the present $N(SO_2F)_2$ group have significant double-bond character, and the lengths are in fact similar to the S–O bond length in SO_2F_2 (1.405 Å), for which a bond order of 2.00 has been assigned.[27] In comparison, the average S–F distance in $FXeN(SO_2F)_2$ (1.535 Å) is the same as the S–F bond length (1.537 (2) Å) of the fluorosulfate anion in $S_6N_4(SO_3F)_2$[23] and the S–F bond length in $FXeOSO_2F$ (1.540 (9) Å)[5] although it is longer than the S–F bond lengths in the $[NSF_2NSO_2F]^-$ anion (1.514 (9) Å average)[17].

It is particularly noteworthy that the bond angles around nitrogen in $FXeN(SO_2F)_2$ are all close to 120° so that the $XeNS_2$ grouping is virtually planar (sum of bond angles 360.1°). The temperature factor for nitrogen is also consistent with it being fairly rigidly held in the molecule. The planar arrangement around nitrogen, as well as the short S–N bond lengths, is also consistent with a significant measure of double-bond character arising from involvement of the nitrogen lone pair in sulfur–nitrogen $p\pi$–$d\pi$ bonding. There is, however, no evidence for restricted rotation about the S–N bonds in solution from our present low-temperature NMR studies. Molecular models indicate that the relative orientations adopted by the SO_2F groups are those that minimize intramolecular repulsions among the oxygen and fluorine atoms of the SO_2F groups. There are a total of three close contacts between the two SO_2F groups: F(11)···O(22), 3.024 Å; F(21)···O(12), 2.960 Å; O(12)···O(22), 3.133 Å. These contacts are only 0.21–0.33 Å greater than the sums of their respective van der Waals radii, indicating the favored conformation is fairly constrained. As a consequence, the molecule possesses a conformation and molecular point group that is not significantly different from C_2. (The deviations of the oxygen and fluorine atoms from the $FXeNS_2$ plane are as follows: F(11), −1.48 Å, F(21), 1.43 Å; O(12), 0.73 Å; O(13), 0.21 Å; O(22), −0.85 Å; O(23), −0.09 Å. Equivalently, this can also be seen in the angles the S–F and S–O bonds make with this plane, viz.: F(11), 43.8°; F(21), 43.0°; O(12), 27.5°; O(13), 8.7°; O(22), 31.2°; O(23), 3.4°.)

The most significant feature of the bond angles at the two sulfur atoms are the large O(12)–S(1)–O(13) and O(22)–S(2)–O(23) bond angles of 123.3 (2) and 121.9 (2)°, respectively. This, again, is consistent with bond–bond repulsions between two sulfur–oxygen bonds possessing considerable double-bond character. This large O–S–O angle distorts the remaining angles around sulfur away from their nominally tetrahedral values so that the average N–S–F, N–S–O, and O–S–F angles are 101.2, 109.2, and 106.3°, respectively. The O–S–O angle is also considerably larger than O–S–O angles of ca. 113–114° in the fluorosulfate anion.[23]

Valence bond structures I and II are consistent with the dimensions of the imidobis(sulfuryl fluoride) ligand and, in particular, the partial double-bond character of the S–N and S–O bonds and the large O–S–O angle.

The arrangement of $FXeN(SO_2F)_2$ molecules in the lattice is illustrated in Figure 2. The closest intramolecular contacts (Table I) are Xe···O(13) and Xe···O(23) of lengths 3.178 (3) and 3.201 (3) Å, respectively. All other intermolecular Xe···O and Xe···F contacts are >3.29 Å in length, and they appear to be avoiding the equatorial region of the F–Xe–N system, presumably due to some lone-pair electron density in that region (F–Xe···O(F) or N–Xe···O(F) angles are <72° or >106° with two exceptions (of 81 and 97°)).

Raman Spectra. The Raman spectrum of $FXeN(SO_2F)_2$ can be satisfactorily assigned on the basis of the observed C_2 point group. Thus, Γ_{vib} = 16 A + 11 B, and all 27 modes are expected to be Raman (and IR) active. A factor-group analysis has also been performed with the site symmetry of the $FXeN(SO_2F)_2$ molecule within the primitive unit cell taken as C_1. The appropriate correlations are given in Table II and predict that each Raman band will be split into A_g and B_g components (A_u and B_u in the IR spectrum) under C_{2h} crystal symmetry. Thus, a maximum of 54 Raman bands could be observed; however, only 36 are actually observed, indicating that the majority of the couplings within the unit cell of $FXeN(SO_2F)_2$ are too small to be resolved.

The assignments for the Raman spectrum of $FXeN(SO_2F)_2$ (Figure 3 and Table III) are based mainly on the assignments for the related $HN(SO_2F)_2$ molecule and $N(SO_2F)_2^-$ anion (cesium salt). Although the vibrational spectra of $HN(SO_2F)_2$ and $N(SO_2F)_2^-$ have been presented previously,[1a,b,24] they were not assigned. We have therefore recorded the Raman spectra of both $HN(SO_2F)_2$ and its cesium salt (Table III) and have made detailed assignments of both systems. The majority of our assignments are based on assignments available for $S_2O_5F_2$,[25] which is isoelectronic with the $N(SO_2F)_2^-$ anion. As in the case of $S_2O_5F_2$, a number of assignments made for the $N(SO_2F)_2$ group are tentative. As it seems likely that $HN(SO_2F)_2$, $N(SO_2F)^-$ and $S_2O_5F_2$ will have staggered conformations (structure III), both systems have been assigned under

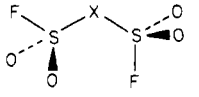

III (X = N⁻, NH, or O)

C_s symmetry (Γ_{vib} = 12 A′ + 9A″). Although $HN(SO_2F)_2$ is expected to possess C_1 symmetry, we have ignored the contribution of the proton to its spectrum (one HN stretch and two HNS bends) for the purpose of our assignments here and have assigned the spectrum of $HN(SO_2F)_2$ under C_s symmetry.

In $FXeN(SO_2F)_2$, nine vibrations may be attributed to the SO_2F group: SO_2 symmetric and asymmetric stretches, an SO_2 bend, two SO_2 rocks, an SF stretch, two SF wags, and an SO_2F torsion (the SO_2 rocking and SF wagging vibrations can occur parallel or perpendicular to the SNS plane). Each of these gives rise to two lines in the spectrum (with coupling between molecules in the unit cell ignored). These are regarded as arising from coupling between the two SO_2F groups, and they are described as in-phase and out-of-phase motions of these groups. Three vibrations may be assigned to the SNS

(23) Gillespie, R. J.; Kent, J. P.; Sawyer, J. F. *Inorg. Chem.* **1981**, *20*, 3784.
(24) Ruff, J. K. *Inorg. Chem.* **1965**, *4*, 1446.
(25) Gillespie, R. J.; Robinson, E. A. *Can. J. Chem.* **1961**, *39*, 2179.
(26) Barnard, D.; Fabian, J. M.; Koch, H. P. *J. Chem. Soc.* **1949**, 2422.
(27) Gillespie, R. J.; Robinson, E. A. *Can. J. Chem.* **1963**, *41*, 2074.

Table II. Raman Frequencies (cm^{-1}) and Tentative Assignments for FXeN(SO$_2$F)$_2$ Compared to Those for HN(SO$_2$F)$_2$, N(SO$_2$F)$_2^-$, and O(SO$_2$F)$_2$[a]

O(SO$_2$F)$_2$[b]	HN(SO$_2$F)$_2$[c]	Cs$^+$N(SO$_2$F)$_2^-$ solid[d]	Cs$^+$N(SO$_2$F)$_2^-$, melt[e]	approx descripn	assignt C_1	FXeN(SO$_2$F)$_2$[d,f] freq	approx descripn	assignt C_2
1511		1376 (6)		SO$_2$ asym str, i	a″	1451 (14), 1449 (24)	SO$_2$ asym str, i	b
	1476 (6), broad		1370 (5) br					
1490		1365 (13)		SO$_2$ asym str, o	a″	1439 (2), 1425 (19)	SO$_2$ asym str, o	b
1264 p	1240 (100) p	1215 (96)	1217 (100) p	SO$_2$ sym str, i	a′	1223 (19), 1216 (20)	SO$_2$ sym str, i	a
1249 p	1218 (11) p	1174 (6)	1174 sh, p	SO$_2$ sym str, o	a′	1209 (10), 1206 sh	SO$_2$ sym str, o	a
872	927 (2)	841 (6)		SNS asym str	a″	888 (33), 881 (11)	SNS asym str	b
814	898 (3)	830 (5)	837 (6)	SF str, i and o	a′, a′	842 (4), 836 (13)	SF str, i, o	a, a
733 p	804 (48) p	727 (15)	734 (67) p	SNS sym str	a′	797 (23), 825 (17)	SNS sym str	a
630	635 (10) p	643 (1)		SO$_2$ bend, o	a′	656 (41)	SO$_2$ bend, o	a
560	569 sh	573 (20)	570 (9)	SO$_2$ ⊥ rock, o	a″	581 (9)	SO$_2$ ⊥ rock, o	b
540	552 (9)	562 (17)		SO$_2$ ⊥ rock, i	a″	559 (8), 551 (7)	SO$_2$ ⊥ rock, i	b
518 p	516 (15)	523 (10)	524 (8) p	SO$_2$ bend, i	a′	514 (6)	SO$_2$ bend, i	a
487	480 (11)	488 (10) 479 (9)	484 (7)	SO$_2$ ∥ rock, i, o	a′, a′	506 (100)	XeF str	a
455 p	463 (13) p	456 (50)	457 (23) p	SF ∥ wag, i	a′	478 (17)	SO$_2$ ∥ rock, i, o	a, a
435	420 (2)	441 (5)		SF ∥ wag, o	a′	469 (17)	SF ∥ wag, i and o	a, a
323 p	323 (66) p	358 (100)	359 (52) p	SNS bend	a′	422 (4)	XeN str	a
366		355 (62)		SO$_2$F torsion, i	a″	340 (52)	SNS bend	a
290	283 (32)	290 (71)	293 (25)	SO$_2$F torsion, o	a″	312 (18)	SF ⊥ wag, i and o	b, b
350		325 (34)		SF ⊥ wag, o	a″	286 (22)	SO$_2$F torsion, i and o	b, b
301	296 sh	329 (28)	328 (18)	SF ⊥ wag, i	a″	220 (113), 215 (87)	FXeN ∥ bend	a
		178 (3)		lattice mode		186 (13), 180 (7)	FXeN ⊥ bend	b
157 p	164 (3) p	156 (8)	168 (6) p	?		141 (43)	lattice mode	
		75 (4)		lattice modes		119 (28), 116 (27)	XeNS ∥ bend	a
		55 (11)				111 (31), 96 (22)	XeNS ⊥ bend	b
						87 (6), 60 sh, 56 (16), 55 sh, 50 (111), 46 (57)	lattice modes	

[a] Raman spectra were recorded in glass sample tubes with use of the 5145-Å exciting line. Values in parentheses denote intensities. Abbreviations: p, polarized line; i, in-phase vibration; o, out-of-phase vibration; ∥, parallel to the SNS (SOS) plane; ⊥, perpendicular to the SNS (SOS) plane. [b] Reference 25. [c] Recorded on the liquid at 25 °C. [d] Recorded at −196 °C. [e] Recorded at 124 °C. [f] Additional weak lines were observed at 1420 (1), 1407 (1), 789 (1), 657 sh, and 651 sh cm^{-1} and are assigned to formally Raman-forbidden A_u and B_u components arising under C_{2h} symmetry of the unit cell. Weak lines at 1001 (2) and 978 (2) cm^{-1} have not been assigned.

Table III. Correlation Diagrams for the Vibrational Modes of $FXeN(SO_2F)_2$[a]

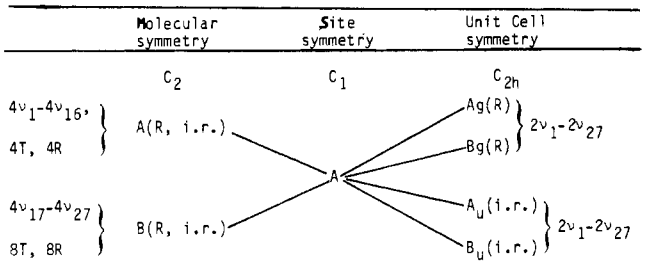

[a] Space group $P2_1/a$ and $Z = 4$. T and R denote translatory and rotatory (external) modes, respectively. R and i.r. in parentheses denote Raman and infrared activity, respectively.

bridging group: a symmetric stretch, an asymmetric stretch, and a bend. Finally, the linear FXeN group is expected to contribute six vibrations: two stretches, an XeF stretch and an XeN stretch, and four bends, in the SNS plane and out of the SNS plane FXeN and XeNS bends.

Frequencies can be readily assigned to the SO_2 stretches, the SO_2 bends, and the SF stretching modes by comparison with the frequencies observed for these vibrations in $S_2O_5F_2$,[25] $N(SO_2F)_2^-$, and $HN(SO_2F)_2$ (Table III). Depolarization measurements on liquid $HN(SO_2F)_2$ and molten $Cs^+N(SO_2F)_2^-$ confirm our assignments of the SO_2 symmetric in-phase and out-of-phase stretches and the in-phase SO_2 bend. The stretching frequencies of the SO_2F group decrease in the series $HN(SO_2F)_2 > FXeN(SO_2F)_2 > N(SO_2F)_2^-$. This is consistent with the anticipated relative contributions of the valence bond structures $X^+N(SO_2F)_2^-$ (X = H, XeF) in which the contribution

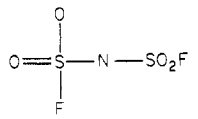

becomes more dominant with increasing ionic character of the N–X bond. The arithmetic mean of the SO_2 stretching frequencies of $FXeN(SO_2F)_2$ can be related to the observed S=O bond length by using the correlations first demonstrated by Barnard, Fabian, and Koch.[26] The predicted S=O bond length, based on data assembled by Gillespie and Robinson,[27] is 1.413 Å compared to the observed mean value of 1.405 (3) Å.

The strong line observed at 340 cm^{-1} for $FXeN(SO_2F)_2$ is assigned to the SNS bending mode, which would be expected to have the lowest frequency of the three skeletal SNS vibrations. The similar SNS and SOS bending frequencies in $HN(SO_2F)_2$ (323 cm^{-1}), $N(SO_2F)_2^-$ (359 cm^{-1}), and $S_2O_5F_2$ (323 cm^{-1}) are also strongly polarized, supporting this assignment. The polarized lines at 804, 727, and 733 cm^{-1} are assigned as the SNS and SOS symmetric stretches in $HN(SO_2F)_2$, $N(SO_2F)_2^-$, and $S_2O_5F_2$, respectively. The corresponding mode in $FXeN(SO_2F)_2$ is assigned to the factor-group split line at 797, 825 cm^{-1} in this region. The asymmetric SNS stretch is expected to have a slightly higher frequency than the symmetric stretch. A depolarized line occurs at approximately 840–925 cm^{-1} in $X(SO_2F)_2$ (X = HN, N^-, or O). Therefore, the factor-group split line at 888, 881 cm^{-1} is assigned to the asymmetric SNS stretch of $FXeN(SO_2F)_2$. The assignments of SNS stretches are supported by the ^{15}N enrichment studies cited later in this discussion.

In the spectra of $X(SO_2F)_2$, there are three groups of lines (excluding the SO_2 bends) between 475 and 575 cm^{-1} which are tentatively assigned to SO_2 rocking modes: the perpendicular out-of-phase, the perpendicular in-phase and the parallel in-phase, and the parallel out-of-phase rocking modes.

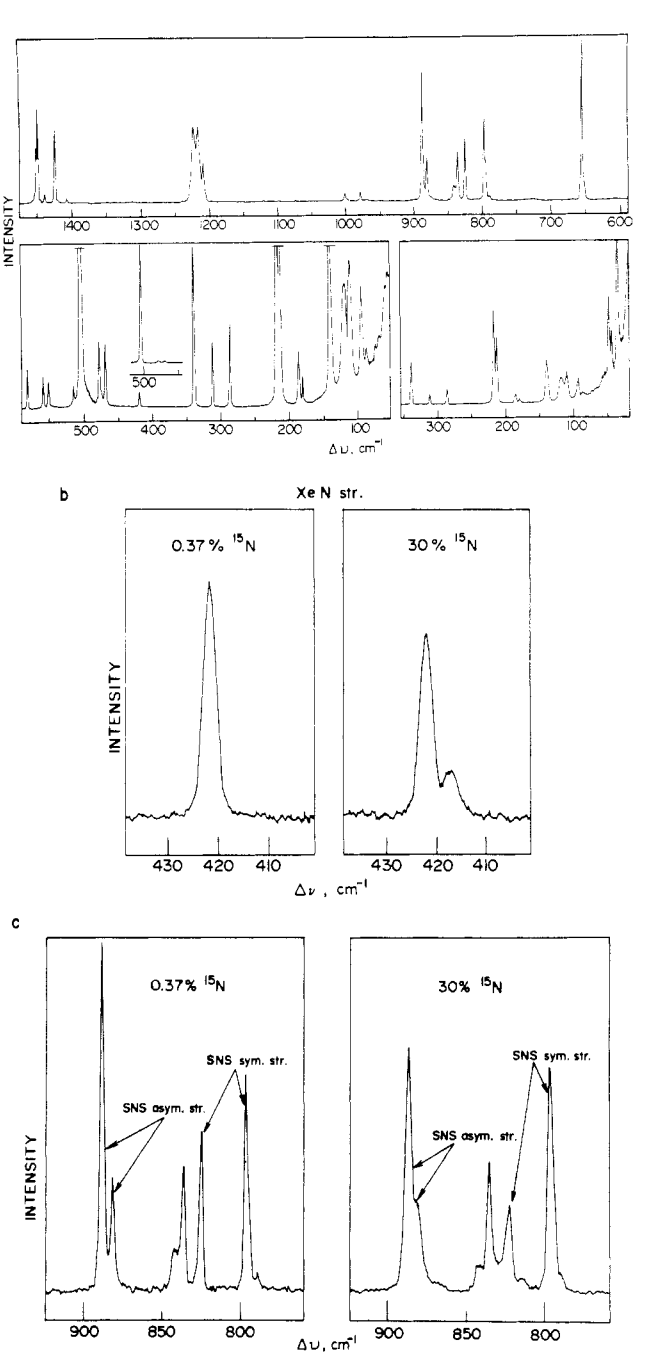

Figure 3. Raman spectra of natural-abundance $FXeN(SO_2F)_2$ recorded at −196 °C (a) and 30% ^{15}N-enriched $FXeN(SO_2F)_2$ showing the isotopic dependencies of the symmetric Xe–N (b) and the factor-group split symmetric and asymmetric S–N–S stretches (c) (the remaining isotopic dependencies are less than the spectrometer resolution of 1 cm^{-1} and are not observed).

Their counterparts occur at 559, 551 (factor-group split) and 581 and 478 (in-phase and out-of-phase components) cm^{-1}, respectively, in $FXeN(SO_2F)_2$.

Although the SF wagging and SO_2F torsional modes in $S_2O_5F_2$ can be used as a guide in the assignment of these modes in $N(SO_2F)_2$ compounds, their in-phase and out-of-phase components as well as the SF wagging motions relative to the skeletal S–O bonds have not been previously specified. It might be anticipated, for example, that the SF wagging mode parallel to an S–N (S–O) bond will occur at higher frequency than that perpendicular to it. We have therefore made specific assignments for all four SF wagging modes and both SO_2F torsions in $XN(SO_2F)_2$ and $FXeN(SO_2F)_2$.

Table IV. NMR Parameters for $FXeN(SO_2F)_2$ and Some Related Compounds

molecule	chemical shift, δ[a]				coupling constant, J, Hz					
	^{129}Xe	^{15}N	^{19}F	^{17}O	^{129}Xe–^{15}N	^{129}Xe–^{19}F	^{129}Xe–$^{19}F'$	^{19}F–^{15}N	$^{19}F'$–^{15}N	^{15}N–^{1}H
$FXeN(SO_2F')_2$[b]	−1997	−250.4	−126.1 (F) 57.6 (F')	169.4	307.4	5586	18.7	39.2		
$(FO_2S)_2N$–$N(SO_2F)_2$[c]		−213.1								
$HN(SO_2F')_2$[d]		−249.2		170.7					7.2	67
XeF_2[e]	−1708		−181.8			5583				

[a] The chemical shift convention is that outlined by IUPAC (*Pure Appl. Chem.* 1972, *29*, 627; 1976, *45*, 217); i.e., a positive chemical shift denotes a positive frequency and vice versa. The following external reference substances were used: ^{129}Xe, neat $XeOF_4$ at 25 °C; ^{15}N, neat CH_3NO_2 at 24 °C, δ^{15}_N (with respect to 7.1 M aqueous NH_4Cl) = δ^{15}_N(with respect to CH_3NO_2) − 359.7 ppm; ^{19}F, neat $CFCl_3$ at −58 °C; ^{17}O, H_2O at 24 °C. [b] 30% ^{15}N enrichment, ~0.5 M in BrF_5 solvent at −58 °C. [c] Decomposition product formed by warming a BrF_5 solution (~0.5 M) of 30% ^{15}N-enriched $FXeN(SO_2F)_2$ to room temperature (see Figure 4c). [d] 30% ^{15}N enrichment, neat sample at 24 °C. [e] 2.70 M in BrF_5 solvent at −40 °C.

As in other compounds containing terminal XeF groups, the XeF stretching mode of $FXeN(SO_2F)_2$ gives rise to the most intense line in the Raman spectrum. This line occurs at 506 cm^{-1} in $FXeN(SO_2F)_2$, which possesses both the longest terminal Xe–F bond (1.967 (3) Å) and the lowest XeF stretching frequency observed to date for an FXeY-type compound (cf. the following: $FXeOTeF_5$, 520 cm^{-1};[28] $FXeOSO_2F$, 528 cm^{-1},[29] 1.940 (8) Å;[5] $(FXeO)_2SOF^+$, 568 cm^{-1},[30] 1.86 (3) Å[7]). Both the terminal Xe–F bond lengths and XeF stretching frequencies of xenon(II) species have been used to assess the relative ionic characters of xenon–ligand bonds. In $FXeN(SO_2F)_2$, the Xe–F bond is only marginally shorter than the Xe–F bonds in XeF_2 (2.01 Å).[11] The slightly greater ionic character of the XeF group in $FXeN(SO_2F)_2$ is also reflected in a comparison of its XeF stretching frequency with the symmetric XeF stretching frequency of XeF_2 (497 cm^{-1}).[31]

A definitive assignment for the XeN stretching frequency has been arrived at by examining the Raman spectrum of 30% ^{15}N-enriched $FXeN(SO_2F)_2$. The weak line found at 422 cm^{-1} displayed a low-frequency shift of 5.2 cm^{-1} (Figure 3b) due to $[^{15}N]FXeN(SO_2F)_2$ and is therefore assigned to the $Xe^{14}N$ stretch. This assignment, when compared to known Xe–O bond lengths and their stretching frequencies in oxygen-bonded xenon(II) species (cf. the following: $FXeOSO_2F$, 434 cm^{-1},[29] 2.155 (8) Å;[5] $Xe(OSO_2F)_2$, 436 cm^{-1};[29] $(FXeO)_2SOF^+$, 398 cm^{-1},[30] 2.21 (2) Å;[7] $Xe(OTeF_5)_2$, 434 cm^{-1};[32] $FXeOTeF_5$, 457 cm^{-1};[28] $XeOTeF_5^+$, 480 cm^{-1};[32] $Xe(OSeF_5)_2$, 550 cm^{-1},[33] 2.12 (5) Å,[12]) is consistent with the observed Xe–N bond length (2.200 (3) Å). The only exception is $Xe(OSeF_5)_2$, which, unlike $Xe(OTeF_5)_2$, has strongly coupled symmetric and asymmetric xenon–oxygen and chalcogen–oxygen stretches involving heavy atoms of widely differing masses.

The isotope (^{15}N) effect on the vibrational frequencies of $FXeN(SO_2F)_2$ appears to be in accordance with the predictions of the Teller–Redlich product rule.[34] In the case of A-type species where only one dependence is clearly resolved, i.e., that for the XeN stretch, and the remaining symmetric SN stretch and symmetric FXeN, XeNS, and SNS bends are assumed to have isotopic dependencies approaching the resolution of the spectrometer (1 cm^{-1}), the observed (and calculated) product of the isotopic frequency ratios $[FXe^{15}N(SO_2F)_2]/[FXe^{14}N(SO_2F)_2]$ is 0.964 (0.967). The agreement between the observed limit and the calculated value is satisfactory and seems to account for our inability to observe other A-type isotopic dependences in the spectrum. Similar arguments may also be made for B-type species where no isotopic dependence is clearly resolved; however, broadening is observed in the bands assigned to the symmetric and asymmetric SN stretches (Figure 3c).

The as yet unassigned low-frequency lines are attributed to FXeN and XeNS bending modes and lattice modes. Bends parallel to the SNS plane are expected to occur at higher frequencies than their perpendicular counterparts. The FXeN bends are anticipated to have frequencies similar to the FXeO bends in the fluorosulfates $FXeOSO_2F$ (239 cm^{-1})[5] and $(FXeO)_2SOF^+$ (242 cm^{-1}).[7] Consequently, these modes are assigned to the moderately strong factor-group split lines at 215, 220 cm^{-1} (parallel) and 180, 186 cm^{-1} (perpendicular). The XeNS bends will occur at lower frequencies than the SNS bend. These modes are assigned to the factor-group split lines at 116, 119 cm^{-1} (parallel) and 96, 111 cm^{-1} (perpendicular). The remaining low-frequency lines are below 90 cm^{-1} and are attributed to lattice modes.

NMR Spectra. Although the ^{19}F NMR spectrum had been cited in the original report of the synthesis of $FXeN(SO_2F)_2$[1a] as evidence for the existence of a Xe–N bond in solution, the interpretation given is not unique. In a subsequent ^{129}Xe NMR study of $FXeN(SO_2F)_2$,[2] it was noted that the previous ^{19}F solution NMR study of $FXeN(SO_2F)_2$ and our ^{129}Xe NMR results could also be interpreted in terms of a structure in which the F–Xe group undergoes at least partial Xe–N ↔ Xe–O bond isomerization with attendant rapid intramolecular exchange of the XeF group over the nitrogen and/or oxygen sites (eq 1).

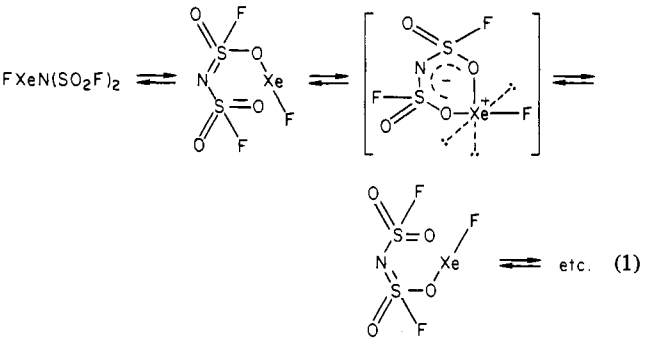

A recent ^{19}F and ^{129}Xe NMR investigation has demonstrated that fluorine-bridged xenon(II) species $FXeF\cdots WOF_4(WOF_4)_n$ (n = 1 or 2) undergo F–Xe–F ↔ F–Xe–O isomerization by means of an XeF group site exchange in solution.[35] We have consequently carried out a detailed multinuclear NMR solution study of $[^{15}N]FXeN(SO_2F)_2$ in BrF_5 as solvent in order to rule out the possibility of intra-

(28) Sladky, F. *Monatsh. Chem.* **1970**, *101*, 1571.
(29) Landa, B.; Gillespie, R. J. *Inorg. Chem.* **1973**, *12*, 1383.
(30) Gillespie, R. J.; Schrobilgen, G. J. *Inorg. Chem.* **1974**, *13*, 1694.
(31) Claassen, H. H.; Goodman, G. L.; Malm, J. G.; Schreiner, F. *J. Chem. Phys.* **1965**, *42*, 1729.
(32) Keller, N.; Schrobilgen, G. J. *Inorg. Chem.* **1981**, *20*, 2118.
(33) Seppelt, K. *Z. Anorg. Allg. Chem.* **1973**, *399*, 87.
(34) Herzberg, G. "Infrared and Raman Spectra of Polyatomic Molecules"; Van Nostrand: New York, 1945; pp 231–238.
(35) Holloway, J. H.; Schrobilgen, G. J. *Inorg. Chem.* **1980**, *19*, 2632.

Table V. Comparison of F–N and F–F′ Reduced Coupling Constants in F–Xe–N$(SO_2F)_2$ and in Compounds Containing F–Ng–F′ (Ng = Kr or Xe) Groups

species	$^2J_{FX}$,[a] Hz	$^2K_{FX}$[a,b]
$FXeF'\cdots MOF_4(MOF_4)_n$[c]	258–275	2.43–2.59
$FXe\cdots F'\cdots XeF^+$	208	1.96
$FKr\cdots F'\cdots KrF^+$	349	3.28
$FKrF'\cdots MOF_4(MOF_4)_n$[d]	296–326	2.78–3.07
$FXeN(SO_2F)_2$	39.2	3.42

[a] X = F′ or N. [b] Reduced coupling constant in units of 10^{20} N A^{-2} m^{-3}. [c] M = Mo, n = 1–3, or M = W, n = 1 or 2. [d] M = Mo, n = 1 or 2, or M = W, n = 0.

molecular exchange and to obtain conclusive evidence for the existence of the Xe–N bond in solution.

The ^{15}N, ^{17}O, ^{19}F, and ^{129}Xe NMR parameters are reported in Table IV. Studies were carried out near the freezing point of the solvent (−58 °C) in order to avoid decomposition of $FXeN(SO_2F)_2$, which occurs at a moderate rate at room temperature according to eq 2. The NMR parameters of the decomposition products are also given in Table IV.

$$2FXeN(SO_2F)_2 \rightarrow XeF_2 + Xe + (FO_2S)_2N{-}N(SO_2F)_2 \quad (2)$$

In addition to the directly bonded ^{129}Xe–^{19}F coupling of the Xe–F group and the three-bond coupling between xenon and the two chemically equivalent fluorines on sulfur observed previously in the ^{129}Xe and ^{19}F spectra[2] (Table IV and Figure 4a,b), two new couplings were observed. The ^{15}N spectrum of 30% ^{15}N-enriched $FXeN(SO_2F)_2$ displays a ^{19}F–^{15}N coupling attributed to a two-bond coupling arising from the terminal fluorine on xenon and the nitrogen (Table IV, Figure 4c). The ^{129}Xe and ^{15}N spectra both display satellites attributed to a directly bonded xenon–nitrogen coupling (Table IV, Figure 4b,c). The relative intensities of the satellites are in agreement with the isotopic abundances of ^{15}N and ^{129}Xe in the samples.

Although the observation of ^{19}F–^{15}N and ^{129}Xe–^{15}N couplings does not, in itself, rule out intramolecular exchange processes, a comparison of the relative sizes of their reduced couplings[36] (see eq 3) does provide evidence for a nonlabile

$$^nK_{AB} = \frac{4\pi^2(^nJ_{AB})}{h\gamma_A\gamma_B} \quad (3)$$

$$^1K_{AB} = \frac{16}{9}\pi\mu_0\mu_B^2\, S_A(0)\, 2S_B(0)^2\, \Pi_{AB} \quad (4)$$

Xe–N bond in solution. A listing of the reduced coupling constants for $FXeN(SO_2F)_2$ is given in Table V. Several examples of nonlabile F–Ng–F′ (Ng = Kr or Xe) systems exist in which fluorine–fluorine spin–spin couplings have been observed in solution. The bonding in the F–Ng–F′ group may be described in terms of the simplified three-center–four-electron bond description used for XeF_2.[12] A comparison of the reduced two-bond coupling constants, $^2K_{FF'}$, for these systems with $^2K_{NF}$ of $FXeN(SO_2F)_2$ is also given in Table V. In cases where multiple bonding is not significant, the Fermi contact contribution is dominant for nuclear spin–spin coupling,[37] and the magnitudes of the reduced one-bond couplings will be influenced, in the main, by the product of the s-electron densities at the coupled centers A and B and the mutual polarizability of the s orbitals on A and B, Π_{AB}, in eq 4, where μ_0 is the permeability of free space and μ_B the Bohr magneton.

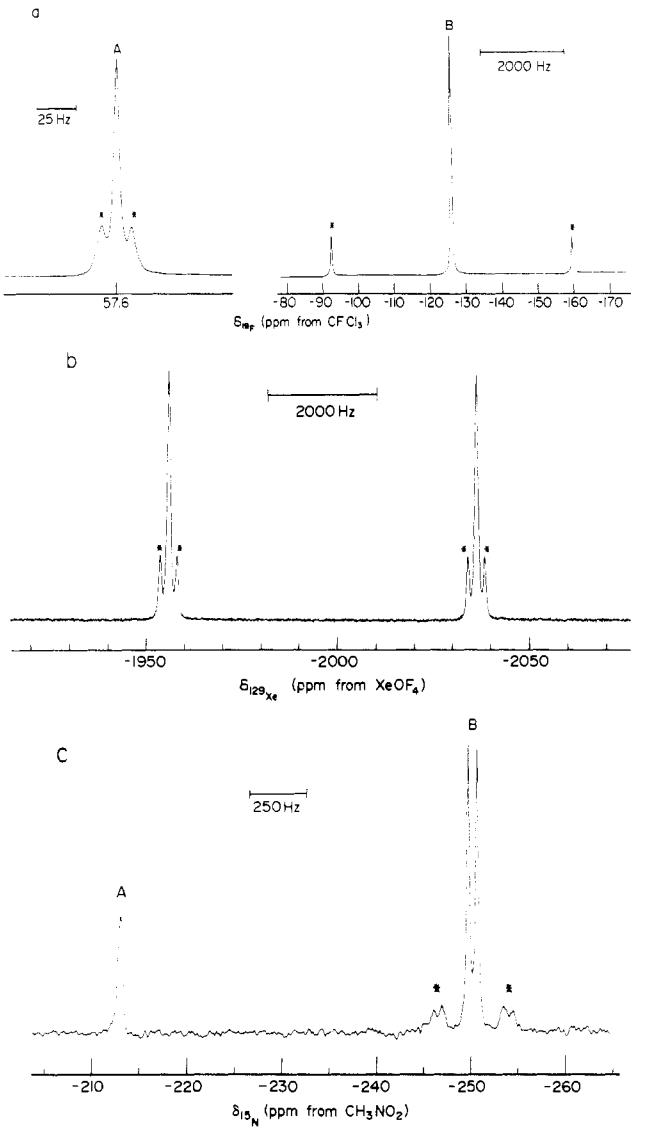

Figure 4. NMR spectra of $FXeN(SO_2F)_2$ (~0.5 M) recorded at −58 °C in BrF_5 solvent: (a) ^{19}F spectrum of the natural-abundance compound showing the fluorines on sulfur, A, and the fluorine on xenon, B, with their respective ^{129}Xe satellites denoted by asterisks; (b) ^{129}Xe spectrum of 30% ^{15}N-enriched $FXeN(SO_2F)_2$, with accompanying ^{15}N satellites denoted by asterisks; (c) ^{15}N spectrum of a partially decomposed sample of 30% ^{15}N-enriched $FXeN(SO_2F)_2$ showing $(FO_2S)_2N{-}N(SO_2F)_2$, A, and $FXeN(SO_2F)_2$, B, with accompanying ^{129}Xe satellites denoted by asterisks.

For nuclei formally separated by more than one chemical bond, a semiempirical approach to the contact term is provided by eq 5, where $S_{S_AS_B}$ is the overlap integral between the valence s orbitals of atoms A and B and the constant is determined experimentally.[37]

$$K_{AB} = \text{constant} \times S_A(0)^2\, S_B(0)^2\, S_{S_AS_B}{}^2 \quad (5)$$

Taking the s-electron densities as the dominant factors for both two-bond couplings and similar overlap integrals, $S_{S_{FF'}} \approx S_{S_{NF}}$, we determined the ratio $^2K_{FF'}/{}^2K_{NF} \approx 2.51$ using the s-electron densities of atomic fluorine and nitrogen[37] in eq 5. The corresponding experimental ratios between F–Ng–F′ systems and F–Xe–N have been evaluated and are significantly smaller, i.e., 0.71–0.96. The low values (large $^2K_{NF}$) appear to result from the greater s-electron character of the sp^2-hybridized orbitals on the nitrogen of $FXeN(SO_2F)_2$ (both fluorines remain sp^3 hybridized in the related F–Ng–F′ systems). From the large experimental value of $^2K_{NF}$ compared to $^2K_{FF'}$ values we may conclude that the observed ^{15}N–^{19}F

(36) Harris, R. K. In "N.M.R. and the Periodic Table"; Harris, R. K., Mann, B. E., Eds.; Academic Press: London, 1978; pp 8–9.
(37) Webb, G. A. In "N.M.R. and the Periodic Table"; Harris, R. K., Mann, B. E., Eds.; Academic Press: London, 1978; pp 62–75.

coupling arises as a result of direct xenon–nitrogen bonding, ruling out fluxional oxygen-bonded intermediates, which would dramatically reduce the total contact contribution to $^2K_{NF}$ and produce high $^2K_{FF'}/^2K_{NF}$ ratios.

A comparison of the reduced coupling constant for the directly bonded Xe–F interaction, $^1K_{XeF} = 17.87 \times 10^{21}$ N A^{-2} m^{-3}, with that for Xe–N, $^1K_{XeN} = 9.13 \times 10^{21}$ N A^{-2} m^{-3}, reveals that, in spite of the effects of sp^2 hybridization at nitrogen, the ratio $K_{XeF}/K_{XeN} = 1.96$ is only somewhat smaller than the ratio calculated from atomic s-electron densities (2.51) by assuming similar mutual polarizabilities in eq 4. The effect of increased s-electron density at nitrogen therefore appears to be largely offset by mutual polarizability differences. The latter can reasonably be expected to parallel relative Xe–F and Xe–N bond orders inferred from the X-ray structure, i.e., $\Pi_{XeF} > \Pi_{XeN}$.

It has been shown that ^{19}F and ^{129}Xe chemical shifts can be used to assess bond ionicities in compounds containing terminal XeF groups. Near-linear correlations exist between the ^{19}F and ^{129}Xe chemical shifts of terminal XeF groups (a low-frequency ^{129}Xe and high-frequency ^{19}F shift signifies an increase in the ionic character of the xenon–ligand atom bond and decrease in the ionic character of the terminal Xe–F bond and vice versa).[2] Compounds containing XeF bonded to another fluorine or to oxygen give two distinct linear correlations with the oxygen-bonded series of Xe–F compounds possessing the smaller absolute slope. When the ^{19}F and ^{129}Xe chemical shifts of $FXeN(SO_2F)_2$ are plotted, they lie on the "oxygen" line and appear to represent, on the basis of this correlation, the most covalent (lowest ^{129}Xe frequency and highest ^{19}F frequency) xenon(II)–ligand atom bond observed to date. The Xe–N bond covalency appears to be greater than that of XeF_2 in the same solvent, BrF_5, at the same temperature (Table IV). This contrasts with the observed Xe–F bond length of $FXeN(SO_2F)_2$, which is actually marginally shorter than those of XeF_2. This discrepancy may arise due to selective solvation effects in the same solvent medium for both compounds. Xenon(II) ^{19}F and ^{129}Xe chemical shifts have been shown to be particularly sensitive to solvation effects.[2] The similarity of $FXeN(SO_2F)_2$ and XeF_2 chemical shifts relative to those of other xenon(II) compounds, however, suggests that the bonding in the F–Xe–N moiety is similar to that in XeF_2 and may therefore reasonably be accounted for in terms of the conventional three-center–four-electron bond model used to describe XeF_2 and related F–Ng–F systems.

The ^{17}O and ^{15}N chemical shifts of $FXeN(SO_2F)_2$ are very similar to those of $HN(SO_2F)_2$ (Table IV). While the similarity of ^{17}O shifts is consistent with our previous contention that Xe–O-bonded contributions in the alternative fluxional interpretation can be ruled out, the insensitivity of the ^{15}N chemical shift for a nitrogen directly bonded to a strongly electron-withdrawing group such as XeF is not readily apparent. The greater inductive effect of the XeF group would be expected to increase the radial factor $\langle r^{-3}\rangle_{2p}$, lower the σ^* HOMO relative to the nonbonding orbital on nitrogen, reducing $\Delta E(n_N \rightarrow \sigma^*)$, and increase ΣQ, the charge-imbalance term for the valence electrons of nitrogen. As all the terms reinforce each other in the expression for the paramagnetic shielding term σ_P^N in eq 6, the net effect would be an increase

$$\sigma_P^N = \frac{-\mu_0\mu_B^2\langle r^{-3}\rangle_{2p}\Sigma Q}{2\pi(\Delta E)} \qquad (6)$$

in the deshielding. However, in $HN(SO_2F)_2$ and $FXeN(SO_2F)_2$ the lone pair of electrons is also part of the π framework and the major paramagnetic contribution to the chemical shift apparently comes from the deshielding of the nitrogen by the $n \rightarrow \pi^*$ circulation of nitrogen lone-pair electrons in π^* orbitals of the sulfur–nitrogen bonds. Apparently this contribution is little influenced by inductive effects of XeF and H, which act through the σ framework and dominates the paramagnetic contributions to ^{15}N chemical shifts in these compounds.

A comparison of ^{129}Xe NMR line widths for $[^{14}N]FXeN(SO_2F)_2$ ($w_{1/2} = 98$ Hz) and $[^{15}N]FXeN(SO_2F)_2$ ($w_{1/2} = 57$ Hz) is also consistent with the Xe–N bonding in solution. The increased line broadening observed for xenon bonded to quadrupolar nitrogen-14 is the result of nearly complete collapse of the ^{129}Xe–^{14}N coupling at −58 °C arising from quadrupole relaxation. The broadness of the ^{129}Xe resonance of $[^{15}N]FXeN(SO_2F)_2$ is in large measure attributable to shielding anisotropy associated with the high-field conditions (5.8719 T) under which these spectra were obtained.

Experimental Section

Apparatus and Materials. All manipulations involving air-sensitive materials were carried out under anhydrous conditions on vacuum lines constructed from 316 stainless steel, nickel, Teflon, and FEP and/or in a drybox. Bromine pentafluoride, arsenic trifluoride, and sulfuryl chlorofluoride were transferred under vacuum through FEP and Teflon connections previously passivated with fluorine. Air-sensitive substances of low volatility, i.e., XeF_2, PCl_5, $HN(SO_2F)_2$, and HSO_3Cl, were transferred in a drybox.

Bromine pentafluoride[32] (Matheson), SO_2ClF[38] (Columbia Organic Chemical), and HSO_3Cl[39] (Eastman) were purified by the standard literature methods. Dichlorodifluoromethane (Matheson) was dried over P_2O_5 prior to use. Phosphorous pentachloride (British Drug Houses), urea (British Drug Houses), [^{15}N]urea (Merck), and sulfamic acid (Aldrich) used in the synthesis of natural-abundance and ^{15}N-enriched $HN(SO_2F)_2$ according to the method of Ruff and Lustig[40] were used without further purification. Sulfamic acid was vacuum-dried at 100 °C overnight and subsequently transferred in a drybox. The preparation of XeF_2 has been described elsewhere.[41]

Arsenic trifluoride, used in the synthesis of $HN(SO_2F)_2$, was prepared by the direct interaction of arsenic powder (K and K Laboratories) with a stoichiometric amount of fluorine (Air Products) at −196 °C followed by heating at 150 °C for 8 h. Prior to fluorination of the arsenic, As_2O_3 surface contaminant was sublimed from the commercial sample of arsenic by heating at 210 °C under vacuum for 2 days. The small amount of AsF_5 also produced in the reaction was rapidly vacuum distilled off at room temperature and the less volatile AsF_3 vacuum distilled onto an excess of NaF (J. T. Baker), previously dried under vacuum at 350 °C for 2 days, in a nickel vessel to remove HF contaminant. After standing for several days, the AsF_3 was vacuum distilled directly into the reaction vessel.

Preparation of $FXeN(SO_2F)_2$ and $[^{15}N]FXeN(SO_2F)_2$. In a typical preparation, 1.89 g (10.4 mmol) of liquid $HN(SO_2F)_2$, prepared and purified according to the methods of Ruff and Lustig,[40] was syringed onto 3.44 g (20.3 mmol) of XeF_2 in a Kel-F vessel (cooled to −196 °C in a drybox). After the cold reaction vessel was equipped with a Kel-F valve, approximately 60 mL of dry CF_2Cl_2 was condensed onto the sample at −196 °C and the sample warmed to 0 °C and vigorously agitated until reaction took place (indicated by liquifaction of $HN(SO_2F)_2$ and dissolution of XeF_2 in this layer to give a dense light yellow immiscible liquid phase). Vigorous agitation was continued until HF formed in the reaction had been extracted into the upper CF_2Cl_2 layer (signified by solidification of the heavier liquid phase into a white powder). After the mixture had stood for 1 day with frequent agitation at 0 °C, CF_2Cl_2 and HF were removed under vacuum at 0 °C. The tube and contents were allowed to warm to room temperature, while they were being pumped, and were pumped on for an additional $1^1/_2$ h at room temperature and 10^{-3} torr to remove excess XeF_2 and subsequently stored at −196 °C until used (yield of $FXeN(SO_2F)_2$ 86%). The sample was shown to be free of excess XeF_2 by low-temperature (−196 °C) Raman spectroscopy.

A procedure identical with that outlined above was used for the preparation of $[^{15}N]FXeN(SO_2F)_2$. Enriched $[^{15}N]HN(SO_2F)_2$ was prepared by the reaction of 7.20 g of ^{15}N-enriched urea (98.4% enriched material was diluted to 30% enrichment with natural-abundance urea) with 100 g of 30% oleum at ~130 °C. After CO_2

(38) Holloway, J. H.; Schrobilgen, G. J. *Inorg. Chem.* **1981**, *20*, 3363.
(39) Barr, J.; Gillespie, R. J.; Thompson, R. C. *Inorg. Chem.* **1964**, *3*, 1149.
(40) Ruff, J. K.; Lustig, M. *Inorg. Synth.* **1968**, *11*, 138.
(41) Williamson, S. M. *Inorg. Synth.* **1968**, *11*, 147.

Table VI. Final Atomic Positional Parameters ($\times 10^4$) for $FXeN(SO_2F)_2$

atom	x	y	z
Xe	1693.3 (2)	6658.5 (3)	1277.0 (2)
S(1)	3124.7 (7)	10154.6 (13)	3755.1 (10)
S(2)	549.0 (7)	10505.5 (12)	2432.1 (9)
F	1593 (3)	4300 (3)	40 (3)
F(11)	3331 (2)	11853 (4)	2813 (3)
F(21)	451 (2)	10006 (4)	3961 (3)
O(12)	3083 (3)	11022 (5)	5056 (3)
O(13)	3985 (3)	8706 (4)	3833 (4)
O(22)	701 (3)	12541 (4)	2421 (3)
O(23)	−437 (2)	9541 (4)	1291 (3)
N	1794 (2)	9355 (4)	2594 (3)

evolution had ceased, heating at 100 °C was continued for an additional 2 h. The mixture was cooled to 0 °C, and 100 mL of H_2O was slowly and cautiously added. The resulting $[^{15}N]H_2NSO_3H$ crystallized from the aqueous H_2SO_4 solution and was filtered off through a coarse glass frit followed by washing with cold CH_3OH. The solid was resuspended in cold diethyl ether and filtered, followed by washing with additional portions of cold diethyl ether. The product was vacuum-dried at room temperature for several days prior to use in the synthetic procedure outlined by Ruff and Lustig.[40]

X-ray Crystallography. Crystals of $FXeN(SO_2F)_2$ suitable for X-ray crystallographic study were grown by dissolution of ca. 0.25 g of pure $FXeN(SO_2F)_2$ in 5 mL of SO_2ClF at room temperature. The sample was cooled to −10 °C and the temperature slowly lowered (2–5 °C/h) until crystallization was complete at −40 °C. The solvent was removed under vacuum at −40 °C, and pumping continued for an additional 2 h at −48 °C. The resulting dry crystals were stored and maintained at −78 °C or below. Some crystals were transferred in a drybox into a cold, dry quartz apparatus equipped with quartz capillary side tubes and manipulated at −10 °C or below. A suitable crystal was tapped into a capillary and was sealed off under an atmosphere of dry nitrogen.

Crystal Data: $XeF_3NO_4S_2$, fw = 330.42, monoclinic, space group $P2_1/a$, a = 11.827 (4) Å, b = 6.828 (2) Å, c = 9.467 (3) Å, β = 112.65 (2)°, V = 705.5 (4) Å^3, D_c = 3.11 g cm^{-3} for Z = 4. Mo K$\bar{\alpha}$ radiation (λ = 0.710 69 Å, μ(Mo K$\bar{\alpha}$) = 56.1 cm^{-1}) was used.

X-ray Intensity Measurements. The crystals decompose in a few hours at room temperature, so all X-ray work was performed at −55 ± 5 °C using a Syntex $P2_1$ diffractometer with an LT-1 low-temperature device.

Intensity data was collected on a small, approximately spherical (R = 0.1 mm, μR = 0.56) colorless crystal sealed in a quartz capillary. Reflections were measured with use of θ–2θ scans over ranges of Kα_1 − 0.9° to Kα_2 + 0.9° with variable scan rates of 2.0–29.3° min^{-1}, which were dependent on the intensity of a prescan. Stationary background counts with a time equal to one-fourth of the scan time for each reflection were made at each end of the scan range. Three standard reflections, which were monitored after every 37 reflections collected, showed no significant variations in intensities over the period of the data collection. A total of 2517 reflections (including standards) in the quadrants (h,k,±l) with $2\theta \leq 60°$ and a further 395 reflections with negative h and k indices were eventually collected.

Lorentz, polarization, and spherical absorption corrections were applied to all data. After equivalent reflections (R_{merge} = 0.022) were averaged and reflections that were systematically absent or had F_{obsd} = 0.0 were excluded, a total of 2002 reflections was obtained and used in the subsequent refinements.

Structure Solution. The structure was solved by the use of the Patterson function to locate the position of the xenon atom. Subsequent cycles of least-squares and Fourier calculations located all the remaining atoms in the structure. Least-squares refinement with all atoms having anisotropic thermal parameters and including a correction for isotropic extinction converged to the agreement indices R_1 = 0.023 and R_2 = 0.030 for 1721 observed ($F > 6\sigma(F)$) reflections and R_1 = 0.027 and R_2 = 0.032 for 1888 reflections with $F > 2\sigma(F)$. In the final cycle of refinement no parameter shifted by more than 18% of its standard error and weights were given by $w^{-1} = \sigma(F)^2 + 0.0003F^2$. The final difference Fourier contained a maximum residual peak of +3.7 e Å^{-3} and a minimum trough of −1.1 e Å^{-3}, close to the xenon atom. The final value of the extinction parameter g as defined by the XRAY system[42] was 1.73 (4) × 10^{-6}.

All calculations were performed on a Cyber computer with the use of the series of programs in the XRAY 76[42] and SHELX systems,[43] as well as some local programs. Neutral-atom scattering factors in the analytical form were taken from ref 44. The final atomic positional parameters are given in Table VI and bond lengths, bond angles, and some significant contact distances in Table I. Final structure factor tables and a listing of anisotropic thermal parameters have been deposited as supplementary material.

Laser Raman Spectroscopy. A Spectra-Physics Model 164 argon ion laser giving up to 900 mW at 5145 Å was used to excite the Raman spectra. The spectrometer was a Spex Industries Model 14018 double monochromator equipped with 1800-grooves/mm holographic gratings. An RCA C31034 phototube detector in conjunction with a pulse count system consisting of pulse amplifier, analyzer, and rate meter (Hamner NA-11, NC-11, and N-708A, respectively) and a Texas Instruments Model FSOZWBA strip-chart recorder were used to record the spectra. The spectrometer was periodically calibrated by recording the discharge lines from an argon lamp over the spectral range of interest; the Raman shifts quoted are estimated to be accurate to ±1 cm^{-1}. Slit widths depended on the scattering efficiency of the sample, laser power, etc., with 1.0 cm^{-1} being typical.

Glass NMR (5-mm o.d.) sample tubes were mounted vertically. The angle between the incident laser beam and the sample tube was 45°, and Raman scattered radiation was observed at 45° to the laser beam (90° to the sample tube axis).

Low-temperature spectra were recorded at −196 °C by mounting the sample vertically in an unsilvered Pyrex glass Dewar filled with liquid nitrogen.

Nuclear Magnetic Resonance. All spectra were recorded on commercial pulse spectrometers and accumulated in 16K of memory with the exception of ^{17}O spectra which were accumulated in 8K of memory. Fluorine-19 spectra were obtained on a Bruker WH-90 spectrometer at 84.66 MHz in 400 scans with a spectral width of 10 kHz (1.2 Hz/data point, 0.815-s pulse acquisition time) and a pulse width of 2 μs. All ^{19}F spectra were deuterium locked with use of a tube of D_2O externally mounted in the probe head; spectra of nuclei other than ^{19}F were obtained on instruments equipped with superconducting magnets and were run unlocked. Xenon-129 and oxygen-17 spectra were obtained at 69.20 and 33.89 MHz, respectively, on a Bruker WM-250 in 800 and 10 000 scans, respectively, at spectral widths of 20 kHz (2.4 (^{129}Xe) and 9.8 (^{17}O) Hz/data point; pulse acquisition times 0.410 (^{129}Xe) and 0.102 s (^{17}O) and pulse widths 20 (^{129}Xe) and 27 (^{17}O) μs). Nitrogen-15 spectra were obtained at 40.55 MHz on a Bruker WH-400 spectrometer in 200–400 scans. The spectral width was 35.7 kHz (4.4 Hz/data point and 0.229-s pulse acquisition time) with a pulse width of 30 μs. A relaxation delay time of 15 s was used in the accumulation of ^{15}N data, and a zero relaxation delay was applied to other nuclei. All spectra were recorded with use of precision thin-wall glass NMR tubes (Wilmad), 5-mm o.d. (^{19}F) and 10-mm o.d. (all other nuclei).

Variable-temperature studies were carried out with use of Bruker temperature controllers. Temperatures were measured with a copper–constantan thermocouple inserted directly into the sample region of the probe and were accurate to ±1 °C.

Acknowledgment. We thank the Natural Sciences and Engineering Research Council of Canada for financial support and the Southwest Ontario Region NMR Center, Guelph, Ontario, for recording the ^{15}N NMR spectra and Bruker Canada, Mississauga, Ontario, for recording the ^{17}O NMR spectra reported in this work.

Registry No. $FXeN(SO_2)_2$, 53719-78-1; $HN(SO_2F)_2$, 14984-73-7; $Cs^+N(SO_2F)_2^-$, 15060-34-1.

Supplementary Material Available: Listings of anisotropic thermal parameters and observed and calculated structure factor amplitudes (12 pages). Ordering information is given on any current masthead page.

(42) "XRAY 76 System of Crystallographic Programs", Technical Report TR-446; Computer Science Center, University of Maryland: College Park, MD, 1976.
(43) Sheldrick, G. M. "SHELX Program for Crystal Structure Determination"; University of Cambridge: Cambridge, England, 1976.
(44) "International Tables for X-ray Crystallography"; Kynoch Press: Birmingham, England, 1965.